Society For Biomaterials

Surface immobilization of MEPE peptide onto HA/β-TCP ceramic particles enhances bone regeneration and remodeling

Bodhraj Acharya,[1] So-Young Chun,[1,2] Shin-Yoon Kim,[3] Cheil Moon,[4] Hong-In Shin,[1] Eui Kyun Park[1]

[1]Department of Pathology and Regenerative Medicine, School of Dentistry, Institute for Hard Tissue and Bio-Tooth Regeneration, Kyungpook National University, Daegu 700-412, Korea
[2]Joint Institute for Regenerative Medicine, Kyungpook National University Hospital, Daegu 700-412, Korea
[3]Department of Orthopaedic Surgery, School of Medicine, Kyungpook National University, Daegu 700-412, Korea
[4]Department of Brain Science, Daegu Gyeongbuk Institute of Science & Technology, Daegu 711-873, Korea

Received 25 May 2011; revised 3 October 2011; accepted 9 October 2011
Published online 25 January 2012 in Wiley Online Library (wileyonlinelibrary.com). DOI: 10.1002/jbm.b.32648

Abstract: Calcium phosphate ceramics have been widely used as scaffolds for bone regeneration. Here, to improve the osteogenic potential of hydroxyapatite/β-tricalcium phosphate (HA/β-TCP) and to apply the bioactive peptide *in situ*, matrix extracellular phosphoglycoprotein (MEPE) peptide, which has been shown to stimulate osteoblast differentiation, was covalently and directionally immobilized on HA/β-TCP particles. The free-hydroxyl groups on the surface of the HA/β-TCP particles were sequentially conjugated with APTES, PEG-$(SS)_2$, and the synthetic MEPE peptide. Using FTIR and XPS, immobilization of the MEPE peptide on the HA/β-TCP was confirmed. Implantation of the MEPE peptide-immobilized HA/β-TCP into calvarial defect and subsequent analyses using a micro CT and histology showed significant bone regeneration and increased bone area (9.89-fold) as compared to that of unmodified HA/β-TCP. Moreover, tartrate-resistant acid phosphatase-positive osteoclasts were observed in regenerated bone by the MEPE peptide-immobilized HA/β-TCP, indicating that the bones newly formed by the MEPE peptide-immobilized HA/β-TCP are actively remodeled by osteoclasts. Therefore, our data demonstrate that MEPE peptide immobilization onto the HA/β-TCP surface stimulates bone regeneration associated with physiological bone remodeling. © 2012 Wiley Periodicals, Inc. J Biomed Mater Res Part B: Appl Biomater 100B: 841–849, 2012.

Key Words: bone regeneration, hydroxyapatite, surface modification, MEPE and bone marrow stem cell

How to cite this article: Acharya B, Chun S-Y, Kim S-Y, Moon C, Shin H-I, Park EK. 2012. Surface immobilization of MEPE peptide onto HA/β-TCP ceramic particles enhances bone regeneration and remodeling. J Biomed Mater Res Part B 2012:100B:841–849.

INTRODUCTION

The implantation of autograft bone remains the preferred reconstructive method but is inadequate for large defect repairs in the craniofacial skeleton because of its limited resources.[1] Synthetic bone graft materials are an alternative to autologous bone, and currently hydroxyapatite (HA)-based ceramics represent the first choice in orthopedic surgery, because they provide an osteoconductivity to which mesenchymal stem cells can migrate and adhere, and can differentiate into functional osteoblasts.[2] HA/β-TCP composite ceramics are widely used because of their biodegradable, biocompatible, and osteoconductive characteristics.[3,4] However, for enhanced bone regeneration they need to be modified.[5] In particular, unlike the natural bone tissues, the synthetic ceramics are mostly pure and lack organic molecules. In the last decade, attention has been focused on producing ceramics effective on osteoconduction and osteoinduction. One of the approaches to improve the performance of HA/β-TCP is the surface immobilization of various peptides and proteins.[5,6] A common covalent linkage method involves grafting a silane group to the hydroxyl groups available at the surface of the ceramics followed by coupling a peptide to the silane group through a bifunctional crosslinker.[5]

MEPE, a noncollagenous acid phosphoprotein, is expressed in osteoblasts, osteocytes and odontoblasts of the bone and dental tissues,[7–9] and regulates bone formation and mineralization.[10–13] It is a member of the small integrin-binding ligand, N-linked glycoprotein (SIBLING) family of secreted glycophosphoproteins.[7,13] Several previous studies have demonstrated that the soluble form of MEPE peptide, AC-100, regulates bone mass and influences osteoblast activity, suggesting its potential for inclusion in novel therapeutic strategies

Additional Supporting Information may be found in the online version of this article.

Correspondence to: E. K. Park; e-mail: epark@knu.ac.kr

Contract grant sponsor: Ministry of Education, Science and Technology, Korea (NRF); contract grant numbers: 2010-0029494, 2010-0020544
Contract grant sponsor: Korea Healthcare technology R&D Project, Ministry for Health, Welfare & Family Affairs, Republic of Korea; contract grant number: A091224
Contract grant sponsor: Fundamental Research Funds for the Central Universities; contract grant number: lzujbky-2012-k12

aimed at increasing osteogenesis.[10,13–15] *In vitro* studies have revealed that the soluble MEPE peptide, mainly AC-100, reserving the RGD and SGDG motifs, enhances the adhesion, spreading, and focal complex formation of osteoblasts, leading to increased osteoblast differentiation and bone formation.[13]

However, for the regeneration of local bone defects commonly caused by trauma or tumor excision, the soluble form of the MEPE peptide may not be suitable because it diffuses out freely when injected. In addition, local bone defects need biomaterials such as calcium phosphate ceramics to fill out the empty space in the defect area. Therefore, in an effort to deliver MEPE peptides efficiently *in situ* and to enhance osteogenic potential of HA/β-TCP ceramic, we immobilized the MEPE peptide on the HA/β-TCP ceramic surface and the *in vivo* bone regeneration was evaluated.

MATERIALS AND METHODS

Materials

HA/β-TCP composite granules were obtained from Zimmer (Germany), 3-aminopropyl-triethoxysilane (APTES) from Sigma-Aldrich (Milwaukee, WI), and polyethylene glycol disuccinimidyl succinate (PEG-$(SS)_2$) from SunBio (Korea). The MEPE peptide (TDLQERGDNDISPFSGDGQP, region 242–261) (95% purity) was synthesized from Peptron (Korea).

Immobilization of the MEPE peptide onto the surface of HA/β-TCP composite particles

HA/β-TCP composite granules were crushed using a mortar, sieved to 250–350 μm and rinsed with ethanol three times. Immobilization of the MEPE peptide involved three different reactions. The first was a silanization to introduce primary amine moieties to the free-hydroxyl group of the HA/β-TCP surface. Briefly, 1 g of the composite particles was soaked in 50 mL of 500 m*M* APTES in anhydrous ethanol for 6 h at 25°C with gentle agitation. For the PEGylation reaction, the silanized particles were rinsed five times with ethanol, then soaked in 50 mL of 2:3 dimethylformamide and ethanol mixture containing 10 m*M* of PEG-$(SS)_2$ for 6 h. The PEGylated HA/β-TCP particles were washed with ethanol and PBS, and then incubated in 50 mL PBS containing 10 μ*M* of synthetic MEPE peptide for 12 h at 4°C with continuous agitation. Then, the particles were washed with PBS and ddH_2O, before being freeze-dried. The particles were hydrated in PBS before implantation. The schematic diagram of the peptide immobilization onto the HA/β-TCP surface is shown in Supporting Information Figure S1.

In vitro osteogenic differentiation of human BMSCs by the synthetic MEPE peptide

To test the *in vitro* osteogenic potential of the synthetic MEPE peptide, human bone marrow stem cells (BMSCs) were isolated as previously described,[16] and seeded at an initial density of 2.5×10^5 cells in a 12-well cell culture plate (Corning, NY), in triplicate, and incubated at 37°C in a humidified atmosphere with 5% CO_2. After 24 h, each well was treated with 1 mL α-MEM with 10% FBS, 1% antibiotics, then supplemented with osteogenic medium containing 0.05 m*M* ascorbic acid, 1 μ*M* dexamethasone, 10 m*M* β-glycerphosphate, and varying concentrations of MEPE peptide (0, 0.47, 2.3, and 4.7 μ*M*).

After 14 days, the cells were washed twice with cold PBS and stained by alizarin red solution (AR-S). The stained dishes were photographed and the stained dye was extracted using 10% cetylpyridinium chloride (CPC) as described previously.[17] Briefly, each well was treated with 400 μL of 10% (w/v) CPC in 10 m*M* sodium phosphate buffer (pH 7.0) and incubated for 30 min at room temperature with gentle shaking. Then, the optical density was measured at 570 nm using a microplate reader (VERSA max, MS Analytical Technologies, PA). Triplicate wells from each case showed the coefficient of variation (CV) to be less than 10%. To analyze the expression of osteoblast differentiation marker genes, total RNA was isolated using TRIzol reagent (Invitrogen, CA). cDNA was synthesized using SuperScript (Invitrogen) with 1 μg of total RNA. The cDNA was normalized with GAPDH and mRNA expression of the osteogenic marker genes osteocalcin (OC), type 1 collagen (COL1), and MEPE by RT-PCR. The sequence of the oligonucleotide primers are listed in Supporting Information Table SI.

To examine the cytotoxicity of the particles, BMSCs were seeded into 96-well plates at a density of 1×10^4 cells/well. Cells were treated with 100 μg particles/well, and cytotoxicity was measured using a CCK-8 kit (Dojindo, Japan), according to the manufacturer's instructions. Optical density at 450 nm was measured with an ELISA plate reader.

Surface characterization of modified HA/β-TCP

The surface properties of the HA/β-TCP composite particles were measured by Fourier transform infrared spectroscopy (FTIR) (Perkin-Elmer Spectrum, GX, MA) and X-ray photoelectron spectroscopy (XPS) (Kratos XSAM-800, UK). Dried PEGlyated and MEPE peptide-immobilized particles were used for IR measurement in KBr disks. A magnesium anode at 20 kV, 10 mA, and a take-off angle of 30° was used. The relative atomic percentage of each element on the surface was estimated from the peak areas using atomic sensitivity factors specified for the photoelectron spectroscopy. Then, X-ray photoelectron spectroscopy (XPS)-C1s spectra bands were deconvoluted into sub-peaks with spectrometer software (XPSPEAK-1.0, UK).

Animal study

Calvarial defects were made in mice by modifying the method described previously.[18,19] Briefly, the ICR mice (male, 5-weeks old) were anesthetized with intramuscular injections of 30 mg/kg of each tiletamine hydrochloride/zolazepam hydrochloride (Zoletil, Virbac animal health, France) and 10 mg/kg of Xylazine hydrochloride (Rumpun, Bayer, Korea). The head was shaved and washed with 70% ethanol. The calvarial bone was exposed by a midline incision of the parietal region and the overlying periosteum was incised. Using a trephine burr on a low-speed dental hand piece (Surgic XT, Nakanishi, Japan) with sterile PBS irrigation, a 4 mm completely circular defect was created on the parietal region. Then, sterile HA/β-TCP particles

(10 mg) were inserted and 5 μL of fibrin glue (Greenplast kit®, Green Cross, Seoul, Korea) was added. The fibrin glue was prepared by a method described earlier.[20] Solution A (2.5 μL) consisting of fibrinogen and a fibrinolyis inhibitor and solution B (2.5 μL) consisting of $CaCl_2$ were added separately in the defect and allowed to clot for 30 s. The fibrin glue held the HA/β-TCP particles together; they were affixed to the surrounding tissue by preventing them from dispersion and movements. The incisions were closed with 3–4 sutures in a single layer. A total of 18 ICR mice were separated into groups of 4, including the control ($n = 3$), unmodified HA/β-TCP ($n = 5$), PEG-$(SS)_2$-immobilized ($n = 5$), and MEPE peptide-immobilized HA/β-TCP ($n = 5$) groups. The animals were sacrificed and the calvaria were harvested 8 weeks post implantation, fixed with 10% formalin, decalcified with 0.5*M* EDTA (pH 8.0) for 4 days, and then embedded in paraffin. The sections were deparaffinized and stained with H&E, Masson's Trichrome and TRAP staining. The bone area was calculated using i-solution software (iMTechnolog, Korea). All animal test procedures were performed in accordance with the specifications of the approved small animal protocol of the Kyungpook National University.

Micro-computed tomography

To analyze the histomorphometric bone regeneration in the calvaria defect, MicroCT imaging was analyzed using X-eye microCT equipment (SEC, Korea), with a maximum tube current of 0.2 MA, a maximum tube volate of 160 kV, and a focus size of 1 μm. The specimens were scanned through 360° at a spatial resolution of 30 μm. The image data from the scanned planes were subsequently thresholded and reconstructed to create 3D images.

RESULTS

In vitro osteogenic activity of the synthetic MEPE peptide

We synthesized MEPE peptides that were three amino acid shorter than AC-100 at the C-terminus for their directional immobilization to HA/β-TCP. Since, the MEPE peptide was immobilized to HA/β-TCP through an amine group at the N-terminus, the lysine residue close to the C-terminus was truncated from the AC-100. Then, we first examined the osteogenic potential of the MEPE peptide. Human BMSCs were treated with the indicated concentration of the MEPE peptide for 2 weeks, and calcium deposition was determined by AR-S staining. As shown in Figure 1(A), mineralization was significantly increased by the MEPE peptide. Quantification of dye extraction also confirmed increased mineral deposition by the MEPE peptide ($p < 0.005$) [Figure 1(B)]. Furthermore, mRNA expression of the osteogenic marker genes such as *OC*, *COL1*, and *MEPE* were increased by the MEPE peptide (0.47 μ*M*) [Figure 1(C)] compared to the control. These results suggest that the MEPE peptide three amino acid shorter than AC-100 stimulates osteogenic differentiation of human BMSCs.

Surface immobilization of MEPEs onto the HA/β-TCP composite particles

Since, the MEPE peptides induced the osteoblast differentiation of human BMSCs, we covalently linked them to the surface of the HA/β-TCP particles for tissue engineering application as described in the Materials and Methods section. To evaluate the immobilization efficiency of MEPE peptides on the HA/β-TCP surface, FTIR (Figure 2), XPS [Figure 3(A)] and XPS-C1s [Figure 3(B), Tables I and II) analyses were conducted. Because of the increase in NH_2, C=C, COO^-, and C=O bonds in the MEPE peptide-immobilized HA/β-TCP, the absorbance peak increased in the respective bond region (1500–1800 cm^{-1}) (Figure 2). Consistent with FTIR results, the MEPE peptide-immobilized HA/β-TCP showed an increase of carbon peaks in the respective bond regions in the XPS-C1s analysis [Figure 3(B) and Table II]. Further, the binding energy for carbon increased in the MEPE peptide-immobilized HA/β-TCP by 26.6% from 3.0 to 3.8 (Table I). On the basis of these results, we confirmed that the MEPE peptide is successfully immobilized to the HA/β-TCP via covalent bonding.

Stimulation of bone regeneration by MEPE peptide in mouse calvarial defect model

To examine the cytotoxic effect of the MEPE peptide-immobilized HA/β-TCP, BMSCs were treated with the indicated particles. When compared to HA/β-TCP or PEG-$(SS)_2$-immobilized HA/β-TCP, the MEPE peptide-immobilized HA/β-TCP showed a similar level of viability for the BMSCs, indicating no significant cytotoxic response of the MEPE peptide-immobilized HA/β-TCP (Supporting Information Figure S2).

To examine the effect of MEPE peptide-immobilized HA/β-TCP on the regeneration of the calvarial defect, the composite particles were implanted as described in the Materials and Methods section. Clinical signs of inflammation or adverse tissue reactions were not observed around the implants. After 8 weeks, the calvaria were scanned with a micro CT. Micro CT image analyses showed, as compared to the control [Figure 4(A)], radiopaque regions in the calvaria where HA/β-TCP [Figure 4(B)], PEG-$(SS)_2$-immobilized HA/β-TCP [Figure 4(C)], and MEPE peptide-immobilized HA/β-TCP [Figure 4(D)] were implanted. Moreover, the coronal sections showed that the margin in the MEPE peptide-immobilized HA/β-TCP [Figure 4(Dc)] case was more regular and continuous than other groups. To determine whether the radiopaque images in the micro CT were due to residual HA/β-TCP particles or new bone formation, the calvaria were decalcified, sectioned, and stained with H&E. The H&E staining results (Figure 5) showed almost no bone regeneration in the control [Figure 5(Aa)] and PEG-$(SS)_2$-immobilized HA/β-TCP [Figure 5(Ac)]. Few initiation centers of bone regeneration were seen in the unmodified HA/β-TCP [Figure 5(Ab)]; whereas almost complete bone regeneration was achieved in the MEPE peptide-immobilized HA/β-TCP cases [Figure 5(Ad)]. Newly formed bone was continuous with the host bone [Figure 5(Ad), black arrow] and the lamination and lacunae were observed [Figure 5(Ad), green arrows], indicating that bone formation is under maturation.

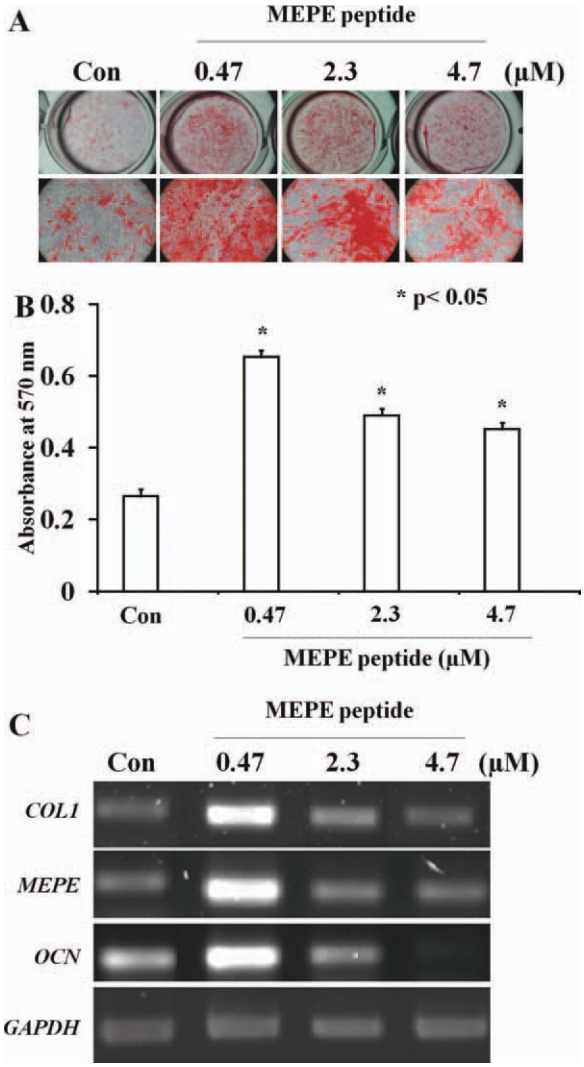

FIGURE 1. *In vitro* effect of the MEPE peptide on mineralization and osteoblast differentiation of human BMSCs. (A) Human BMSCs were treated with the indicated concentration of MEPE peptide for 2 weeks, and stained with alizarin red S. (B) The stained dye was extracted with using 10% CPC, and the optical density at 570 nm was measured. (C) BMSCs were treated with the indicated concentration of MEPE peptide for 2 weeks, and the expression of osteoblast differentiation maker genes was measured by RT-PCR; *COL1*; Collagen type 1, MEPE; Matrix extracellular phosphoglycoprotein and OCN; Osteocalcin. [Color figure can be viewed in the online issue, which is available at wileyonlinelibrary.com.]

The HA/β-TCP was found to be remaining in all three groups for 8 weeks (open arrows). To quantify the newly formed bone, the bone area was measured using i-solution software. The results showed that bone regeneration in the MEPE peptide-immobilized HA/β-TCP cases was significantly higher ($p = 0.002157$) than the unmodified HA/β-TCP cases [Figure 5(B)].

To further confirm bone formation and maturation, a Masson's Trichrome staining was performed. When compared to the control [Figure 6(A)], HA/β-TCP [Figure 6(B)], and PEG-$(SS)_2$-immobilized HA/β-TCP [Figure 6(C)] groups, much thicker mature bone (red color) was seen in the MEPE peptide-immobilized HA/β-TCP group [Figure 6(D)]. In addition, in the MEPE peptide-immobilized HA/β-TCP group, immature bone (osteoid) was detected around the particles (blue color; green arrows), and much less immature bone in the HA/β-TCP group, indicating that the MEPE peptide-immobilized HA/β-TCP supports active bone maturation following bone formation.

To examine whether the newly formed bone was remodeled, the sections were stained with TRAP, which reflects the presence of osteoclasts. When compared to HA/β-TCP (Figure 7(B)] and PEG-$(SS)_2$-immobilized HA/β-TCP [Figure 7(C)], TRAP-positive multinucleated cells were present in the newly formed bone around the MEPE peptide-immobilized HA/β-TCP [Figure 7(D)], indicating that newly formed bone is actively remodeled by osteoclasts.

Taken together, these results demonstrate that bone regeneration was efficiently enhanced by the MEPE peptide-immobilized HA/β-TCP, and the newly formed bone is under physiological remodeling.

DISCUSSION

Of the calcium phosphate ceramics, HA/β-TCP composite has been shown to be the most useful in bone regeneration because of its biodegradability and osteoconductivity in the body. Although, the biodegradability of HA/β-TCP has been improved, it still lacks organic materials such as an

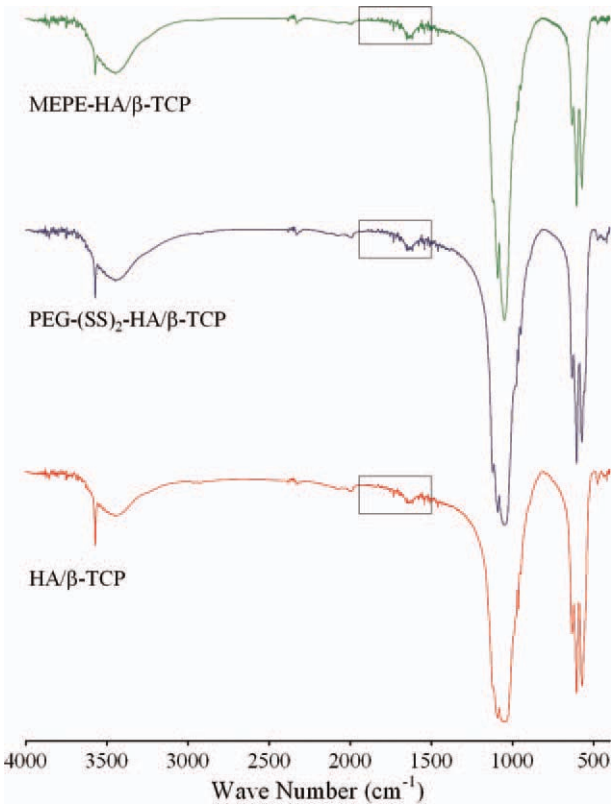

FIGURE 2. FTIR analysis. Absorption peaks of the HA/β-TCP, PEG-$(SS)_2$-immobilized HA/β-TCP, and MEPE peptide-immobilized HA/β-TCP were measured using FTIR. Increased stretching (boxed) is seen in the MEPE peptide-immobilized HA/β-TCP due to peptide immobilzation. [Color figure can be viewed in the online issue, which is available at wileyonlinelibrary.com.]

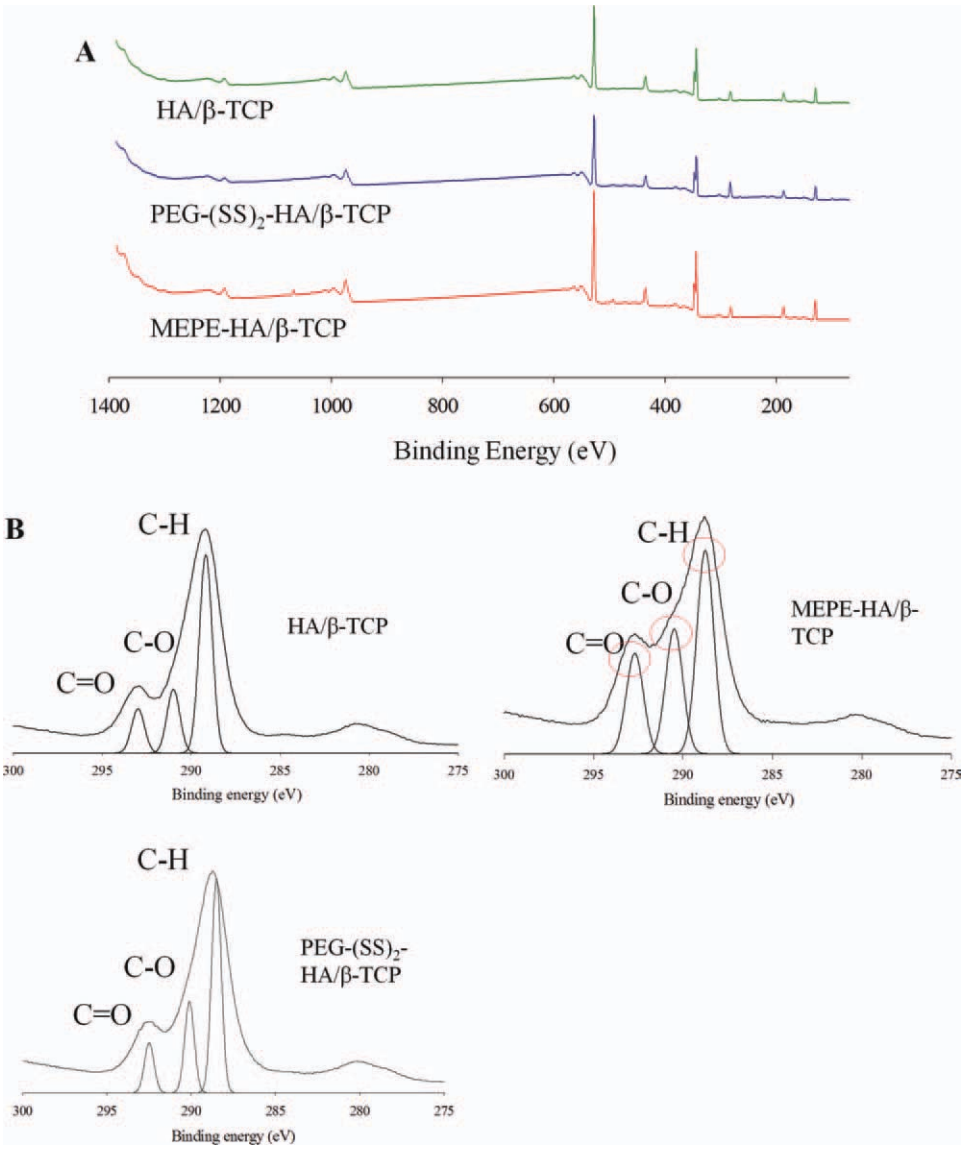

FIGURE 3. XPS analysis. (A) XPS spectra of unmodified HA/β-TCP, PEG-$(SS)_2$-immobilized HA/β-TCP and MEPE peptide-immobilized HA/β-TCP. (B) XPS-C1s spectra for MEPE peptide-immobilized HA/β-TCP, unmodified HA/β-TCP, and PEG-$(SS)_2$-immobilized HA/β-TCP. [Color figure can be viewed in the online issue, which is available at wileyonlinelibrary.com.]

extracellular matrix or bioactive proteins, which appear in natural bone. Therefore, the conjugation or less effectively, the addition of HA/β-TCP with bioactive proteins may strongly enhance osteoconduction or osteointegration with a host bone. Surface immobilization of bioactive proteins to HA/β-TCP can be achieved by consecutive chemical reactions targeting amine moiety. APTES has been used as a spacer molecule with HA,[5,21,22] and disuccinimidyl succinate reacts with amine group, and thus covalently binds to molecules containing primary amines.[23] We found that the linkers APTES and PEG-$(SS)_2$ efficiently bind the MEPE peptide

TABLE I. Increase in the Binding Energy of Carbon from MEPE Peptide-Immobilized HA/β-TCP

	Binding Energy (ev)		
	HA/β-TCP	PEG-$(SS)_2$-Immobilized HA/β-TCP	MEPE-Immobilized HA/β-TCP
O	2.8	3.3	2.8
Ca	2.7	2.6	2.5
C	3.0	2.9	3.8
P	2.8	2.7	2.6

O, oxygen; Ca, calcium; C, carbon; P, phosphorous.

TABLE II. XPS Results of C=O and C—H bond percentage increase

Groups	C=O/C—H Ratio (%)
HA/β-TCP	23.97
PEG-$(SS)_2$-immobilized HA/β-TCP	25.66 ± 1.09
MEPE-immobilized HA/β-TCP	48.42 ± 3.27

O, oxygen; C, carbon; H, hydrogen.

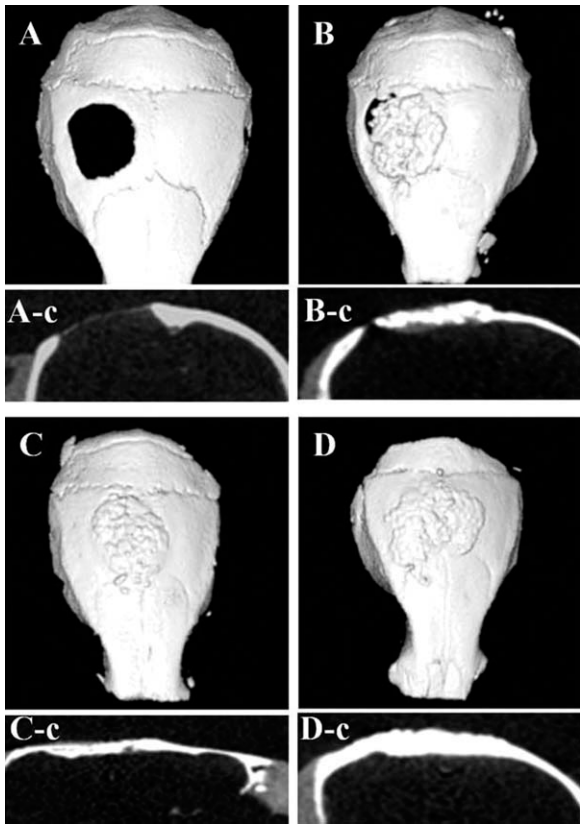

FIGURE 4. MicroCT analysis of mouse calvaria. Eight weeks after implantation, 3D images of mouse calvaria were obtained using microCT; (A) control without HA/β-TCP, (B) unmodified HA/β-TCP, (C) PEG-$(SS)_2$-immoblized HA/β-TCP, and (D) MEPE peptide-immobilized HA/β-TCP. Coronal section images of (A-c) untreated control, (B-c) unmodified HA/β-TCP, (C-c) PEG-$(SS)_2$-immobilized HA/β-TCP, and (D-c) MEPE-immobilized HA/β-TCP were shown from the top view images.

to the surface of HA/β-TCP (Figures 2 and 3). Although, we could not determine the immobilization efficiency, our data demonstrate that the MEPE peptide was successfully immobilized on the surface of the HA/β-TCP particles (Figures 2 and 3).

Surface immobilization of bioactive molecules such as growth factors and peptides may stimulate cell responses as compared to their soluble form.[24] For example, tethered epidermal growth factor (EGF) increases the spread and survival of MSC more strongly than soluble EGF through sustained activation of the ERK signaling.[24] Immobilized EGF inhibits EGF receptor internalization and degradation, and thus prevents the downregulation of the EGF receptor.[25,26] Similarly, since the MEPE peptide contains an RGD motif, the integrins responsible for RGD binding may not be internalized and degraded, and consequently integrin signaling may be activated and sustained. This may explain the enhanced bone regeneration by the MEPE peptide-immobilized HA/β-TCP as compared to the unmodified and PEG-$(SS)_2$-immobilized HA/β-TCP (Figures 5 and 6).

Absorbed molecules are not guaranteed to elicit a sustained cellular response during bone regeneration whereas covalently bound molecules have a longer retention time after implantation, and they remain on the surface until acted upon by cell interactions.[5] Therefore, although we do not have evidence regarding the release of the MEPE peptide here, it can be easily speculated that the MEPE peptide is slowly released from HA/β-TCP over time in the implanted calvarial area, and the sustained release of the MEPE peptide may also have induced comparative bone regeneration.

Enhanced bone regeneration by the surface modified HA/β-TCP may be achieved by the characteristics of the peptide that has been immobilized. Since, the MEPE peptide contains RGD and SGDG motifs, it can stimulate integrins and promote glycosaminoglycan (GAG) attachment. In fact,

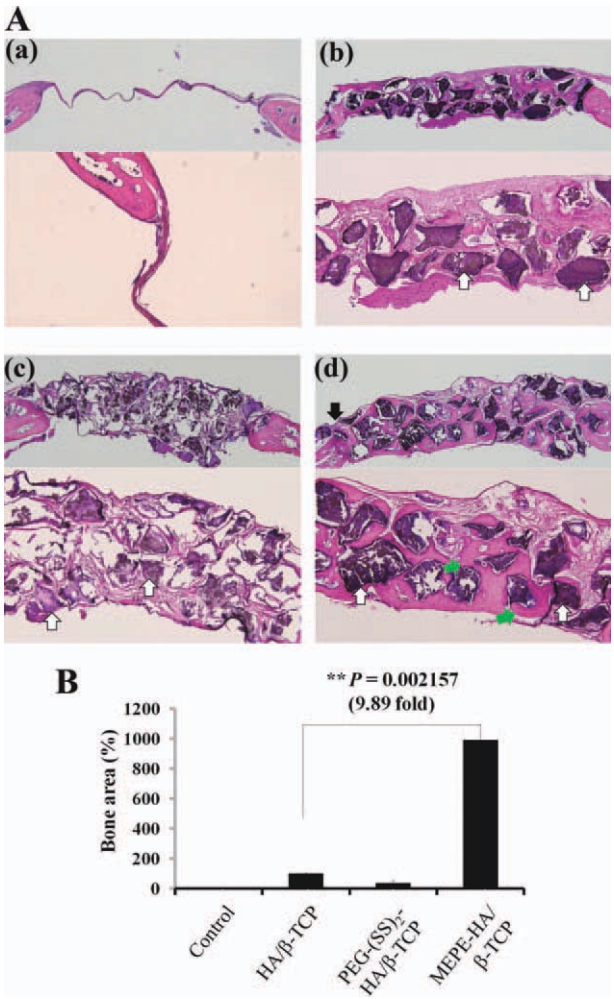

FIGURE 5. H&E staining and bone area measurement. Eight weeks after implantation, the calvaria were sectioned and stained with H&E staining; (A-a) defect without HA/β-TCP, (A-b) unmodified HA/β-TC, (A-c) PEG-$(SS)_2$-immobilized HA/β-TCP, and (A-d) MEPE peptide-immobilized HA/β-TCP. Lower magnification images (×50) of each group were shown in the upper panel and higher magnification images (×100) were shown in the lower panel. The newly formed bone is shown with green arrows, the region where new bone and host bone have fused are indicated with a black arrow, and remaining HA/β-TCP ceramics were indicated with open arrows. (B) The area of newly formed bone was measured using i-solution software. $p = 0.002157$. [Color figure can be viewed in the online issue, which is available at wileyonlinelibrary.com.]

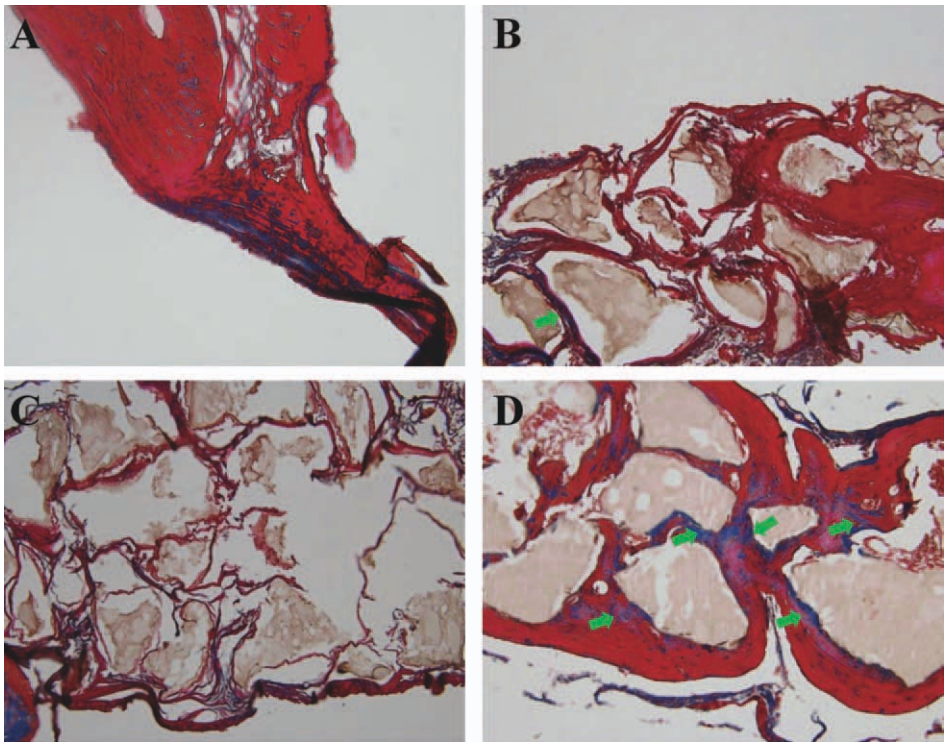

FIGURE 6. Masson's Trichrome staining. Calvarial sections of (A) defect without HA/β-TCP, (B) unmodified HA/β-TCP, (C) PEG-$(SS)_2$-immobilized HA/β-TCP, and (D) MEPE peptide-immobilized HA/β-TCP were stained with Masson's Trichrome staining. Green arrows indicate matured bone, and the red colored region represents the osteoid. Magnification: ×200. [Color figure can be viewed in the online issue, which is available at wileyonlinelibrary.com.]

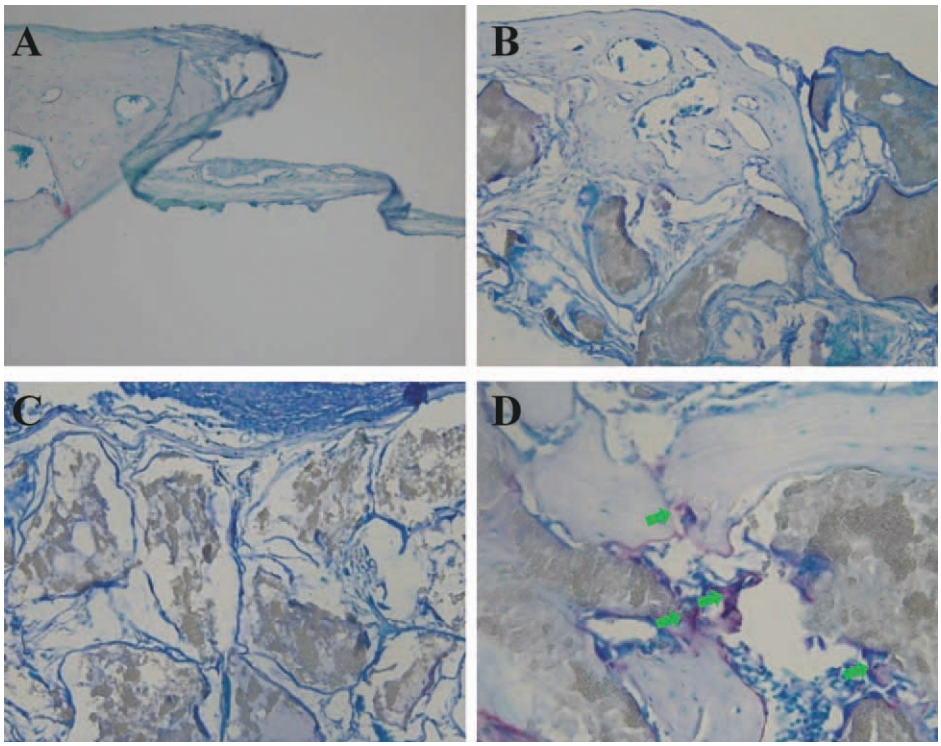

FIGURE 7. TRAP staining. Calvarial sections of (A) defect without HA/β-TCP, (B) unmodified HA/β-TCP, (C) PEG-$(SS)_2$-immobilized HA/β-TCP, and (D) MEPE peptide-immobilized HA/β-TCP were stained with TRAP. Multinucleated osteoclastic cells were seen in MEPE peptide-immobilized HA/β-TCP (green arrows) whereas no osteoclastic activity were seen in control, unmodified HA/β-TCP or PEG-$(SS)_2$-immobilzied HA/β-TCP. Magnification: ×200. [Color figure can be viewed in the online issue, which is available at wileyonlinelibrary.com.]

an RGD motif has been shown to enhance implant osteointegration and positively affect the bone-bonding ability of porous implants,[27] and various approaches for RGD conjugation and its efficiency have been reported.[21,23,28–31] RGD conjugated materials promote adhesion, proliferation, and collagen secretion of human fibroblasts[6] through integrins[22] and its binding to integrin leads to the activation of cascades of cytoplasmic signaling pathways and gene transcription.[32] Osteoblasts express various types of integrins that can interact with the RGD motif.[33] However, high concentration of soluble peptide blocks the peptide-mediated cellular responses.[34,35] Binding of excess soluble RGD peptide to integrin fails to stimulate integrin signaling, and rather can block integrin signaling elicited by other extracellular matrix proteins containing RGD motif or the peptide attached to a scaffold or culture dish. Therefore, a low-concentration of the soluble MEPE peptide may show a maximum increase of mineralization and gene expression of osteoblast differentiation through RGD motif whereas increasing concentration of the soluble MEPE peptide may partially reduce these responses (Figure 1). In contrast, conjugation of the MEPE peptide enhanced HA/β-TCP incorporation in the host tissue as revealed by microCT imaging and H&E staining [Figures 4(Dc) and 5(Ad)], which lead to effective bone regeneration [Figures 5(Ad) and (6D)]. The SGDG motif in the MEPE peptide is responsible for GAG attachment. GAG sugars are responsible for the various bioactivities of proteoglycan proteins. Particularly, it is important for mediating the processes of cell attachment and growth factor signaling.[36] Therefore, enhanced bone regeneration by the MEPE peptide-immobilized HA/β-TCP may be achieved through the direct activation of osteoblasts through integrins or GAG attachment as well as sustained release of the peptides.

For physiological bone regeneration, bone remodeling by osteoclasts is also needed. We observed comparative osteoclastic activity in the MEPE peptide-immobilized HA/β-TCP group (Figure 7). Osteoclasts play an important role in bone remodeling by closely cooperating with osteoblasts to optimize bone structure and alignment.[37] Moreover, not only the bone but also the implanted biomaterial needs to be reabsorbed during bone regeneration. As with the other implanted materials, calcium phosphates are resorbed by several mechanisms. A portion of the material may dissolve in the surrounding biologic milieu or cell-mediated processes occur as osteoclasts directly resorb foreign materials.[38] Therefore, the osteoclastic activity that was seen in the MEPE peptide-immobilized cases [Figure 7(D)] might play an important role in the remodeling of the newly formed bone and lead to effective bone regeneration. Collectively, our data strongly suggest that MEPE peptide immobilization on HA/β-TCP contributes to the stimulation of bone regeneration in the calvaria defect model with physiological bone remodeling.

CONCLUSION

This is the first report to successfully immobilize the MEPE peptide containing RGD and SGDG motifs onto the surface of HA/β-TCP. The MEPE peptide-immobilized HA/β-TCP significantly enhances bone regeneration in the calvaria defect model with physiological bone remodeling. Therefore, immobilization of the bioactive peptide on ceramics may be useful in improving the osteogenic potential of biomaterials.

REFERENCES

1. Mankani MH, Kuznetsov SA, Wolfe RM, Marshall GW, Robey PG. In vivo bone formation by human bone marrow stromal cells: reconstruction of the mouse calvarium and mandible. Stem Cells 2006;24:2140–2149.
2. Paderni S, Terzi S, Amendola L. Major bone defect treatment with an osteoconductive bone substitute. Chir Organi Mov 2009;93: 89–96.
3. Lu X, Li S, Zhang J, Zhang Z, Lu B, Bu H, Li Y, Cheng J. Biocompatibility of HA/TCP biphasic ceramics with co-cultured human osteoblasts in vitro. Sheng Wu Yi Xue Gong Cheng Xue Za Zhi 2001;18:497–499.
4. Macchetta A, Turner IG, Bowen CR. Fabrication of HA/TCP scaffolds with a graded and porous structure using a camphene-based freeze-casting method. Acta Biomater 2009;5:1319–1327.
5. Wang V, Misra G, Amsden B. Immobilization of a bone and cartilage stimulating peptide to a synthetic bone graft. J Mater Sci Mater Med 2008;19:2145–2155.
6. Li B, Chen J, Wang JH. RGD peptide-conjugated poly(dimethylsiloxane) promotes adhesion, proliferation, and collagen secretion of human fibroblasts. J Biomed Mater Res A 2006;79:989–998.
7. Gluhak-Heinrich J, Pavlin D, Yang W, MacDougall M, Harris SE. MEPE expression in osteocytes during orthodontic tooth movement. Arch Oral Biol 2007;52:684–690.
8. Liu H, Li W, Gao C, Kumagai Y, Blacher RW, DenBesten PK. Dentonin, a fragment of MEPE, enhanced dental pulp stem cell proliferation. J Dent Res 2004;83:496–499.
9. Rowe PS, Kumagai Y, Gutierrez G, Garrett IR, Blacher R, Rosen D, Cundy J, Navvab S, Chen D, Drezner MK, Quarles LD, Mundy GR. MEPE has the properties of an osteoblastic phosphatonin and minhibin. Bone 2004;34:303–319.
10. Addison WN, Nakano Y, Loisel T, Crine P, McKee MD. MEPE-ASARM peptides control extracellular matrix mineralization by binding to hydroxyapatite: An inhibition regulated by PHEX cleavage of ASARM. J Bone Miner Res 2008;23:1638–1649.
11. Argiro L, Desbarats M, Glorieux FH, Ecarot B. Mepe, the gene encoding a tumor-secreted protein in oncogenic hypophosphatemic osteomalacia, is expressed in bone. Genomics 2001;74: 342–351.
12. Nampei A, Hashimoto J, Hayashida K, Tsuboi H, Shi K, Tsuji I, Miyashita H, Yamada T, Matsukawa N, Matsumoto M, Morimoto S, Ogihara T, Ochi T, Yoshikawa H. Matrix extracellular phosphoglycoprotein (MEPE) is highly expressed in osteocytes in human bone. J Bone Miner Metab 2004;22:176–184.
13. Sprowson AP, McCaskie AW, Birch MA. ASARM-truncated MEPE and AC-100 enhance osteogenesis by promoting osteoprogenitor adhesion. J Orthop Res 2008;26:1256–1262.
14. David V, Martin A, Hedge AM, Rowe PS. Matrix extracellular phosphoglycoprotein (MEPE) is a new bone renal hormone and vascularization modulator. Endocrinology 2009;150:4012–4023.
15. Hayashibara T, Hiraga T, Yi B, Nomizu M, Kumagai Y, Nishimura R, Yoneda T. A synthetic peptide fragment of human MEPE stimulates new bone formation in vitro and in vivo. J Bone Miner Res 2004;19:455–462.
16. Park EK, Lee YE, Choi JY, Oh SH, Shin HI, Kim KH, Kim SY, Kim S. Cellular biocompatibility and stimulatory effects of calcium metaphosphate on osteoblastic differentiation of human bone marrow-derived stromal cells. Biomaterials 2004;25:3403–3411.
17. Lee SY, Lim J, Khang G, Son Y, Choung PH, Kang SS, Chun SY, Shin HI, Kim SY, Park EK. Enhanced ex vivo expansion of human adipose tissue-derived mesenchymal stromal cells by fibroblast growth factor-2 and dexamethasone. Tissue Eng Part A 2009;15: 2491–2499.
18. Cowan CM, Shi YY, Aalami OO, Chou YF, Mari C, Thomas R, Quarto N, Contag CH, Wu B, Longaker MT. Adipose-derived adult stromal cells heal critical-size mouse calvarial defects. Nat Biotechnol 2004;22:560–567.

19. Osathanon T, Linnes ML, Rajachar RM, Ratner BD, Somerman MJ, Giachelli CM. Microporous nanofibrous fibrin-based scaffolds for bone tissue engineering. Biomaterials 2008;29:4091–4099.
20. Hafeli UO, Pauer GJ, Unnithan J, Prayson RA. Fibrin glue system for adjuvant brachytherapy of brain tumors with 188Re and 186Re-labeled microspheres. Eur J Pharm Biopharm 2007;65:282–288.
21. Durrieu MC, Pallu S, Guillemot F, Bareille R, Amedee J, Baquey CH, Labrugere C, Dard M. Grafting RGD containing peptides onto hydroxyapatite to promote osteoblastic cells adhesion. J Mater Sci Mater Med 2004;15:779–786.
22. Yang C, Cheng K, Weng W. Immobilization of RGD peptide on HA coating through a chemical bonding approach. J Mater Sci: Mater Med 2009;20:2349–2352.
23. Tessmar JK, Mikos AG, Gopferich A. Amine-reactive biodegradable diblock copolymers. Biomacromolecules 2002;3:194–200.
24. Fan VH, Tamama K, Au A, Littrell R, Richardson LB, Wright JW, Wells A, Griffith LG. Tethered epidermal growth factor provides a survival advantage to mesenchymal stem cells. Stem Cells 2007; 25:1241–1251.
25. Chen WS, Lazar CS, Lund KA, Welsh JB, Chang CP, Walton GM, Der CJ, Wiley HS, Gill GN, Rosenfeld MG. Functional independence of the epidermal growth factor receptor from a domain required for ligand-induced internalization and calcium regulation. Cell 1989;59:33–43.
26. Wiley HS. Trafficking of the ErbB receptors and its influence on signaling. Exp Cell Res 2003;284:78–88.
27. Yang GL, He FM, Yang XF, Wang XX, Zhao SF. In vivo evaluation of bone-bonding ability of RGD-coated porous implant using layer-by-layer electrostatic self-assembly. J Biomed Mater Res A 2009;90:175–185.
28. Bitschnau A, Alt V, Bohner F, Heerich KE, Margesin E, Hartmann S, Sewing A, Meyer C, Wenisch S, Schnettler R. Comparison of new bone formation, implant integration, and biocompatibility between RGD-hydroxyapatite and pure hydroxyapatite coating for cementless joint prostheses—An experimental study in rabbits. J Biomed Mater Res B Appl Biomater 2009;88:66–74.
29. Hennessy KM, Clem WC, Phipps MC, Sawyer AA, Shaikh FM, Bellis SL. The effect of RGD peptides on osseointegration of hydroxyapatite biomaterials. Biomaterials 2008;29:3075–3083.
30. Itoh D, Yoneda S, Kuroda S, Kondo H, Umezawa A, Ohya K, Ohyama T, Kasugai S. Enhancement of osteogenesis on hydroxyapatite surface coated with synthetic peptide (EEEEEEEPRGDT) in vitro. J Biomed Mater Res 2002;62:292–298.
31. Okamoto K, Matsuura T, Hosokawa R, Akagawa Y. RGD peptides regulate the specific adhesion scheme of osteoblasts to hydroxyapatite but not to titanium. J Dent Res 1998;77:481–487.
32. Giancotti FG, Ruoslahti E. Integrin signaling. Science 1999;285: 1028–1032.
33. Damsky CH. Extracellular matrix-integrin interactions in osteoblast function and tissue remodeling. Bone 1999;25:95–96.
34. Tosatti S, Schwartz Z, Campbell C, Cochran DL, VandeVondele S, Hubbell JA, Denzer A, Simpson J, Wieland M, Lohmann CH, Textor M, Boyan BD. RGD-containing peptide GCRGYGRGDSPG reduces enhancement of osteoblast differentiation by poly(L-lysine)-graft-poly(ethylene glycol)-coated titanium surfaces. J Biomed Mater Res A 20041;68:458–472.
35. Shin H, Zygourakis K, Farach-Carson MC, Yaszemski MJ, Mikos AG. Modulation of differentiation and mineralization of marrow stromal cells cultured on biomimetic hydrogels modified with Arg-Gly-Asp containing peptides. J Biomed Mater Res A 2004;69: 535–543.
36. Kumarasuriyar A, Lee I, Nurcombe V, Cool SM. De-sulfation of MG-63 cell glycosaminoglycans delays in vitro osteogenesis, up-regulates cholesterol synthesis and disrupts cell cycle and the actin cytoskeleton. J Cell Physiol 2009;219:572–583.
37. Schell H, Lienau J, Epari DR, Seebeck P, Exner C, Muchow S, Bragulla H, Haas NP, Duda GN. Osteoclastic activity begins early and increases over the course of bone healing. Bone 2006;38: 547–554.
38. Wang W, Ferguson DJ, Quinn JM, Simpson AH, Athanasou NA. Biomaterial particle phagocytosis by bone-resorbing osteoclasts. J Bone Joint Surg Br 1997;79:849–856.